HYDROLOGY OF SCAMANDER VALLIS, MARS. Christopher Coughenour and Neil Coleman, University of Pittsburgh at Johnstown (Dept. of Energy & Earth Resources, Johnstown, PA 15904; coughenour@pitt.edu).

Introduction: Evidence of early hydrologic activity is preserved in the Noachian terrains of Mars, most of which are highlands. Compared to later periods, the Noachian reveals evidence of high rates of impact cratering, erosion and weathering, and formation of valley networks [1]. Davis et al. [2] examine the depositional history of these systems in Arabia Terra and conclude that rivers and lakes evolved in Arabia Terra during prolonged and episodic precipitation. The postulated water inventories that likely existed would have supported oceans or seas in lowlands like the northern plains and Hellas basin. Here we examine Scamander Vallis, which appears to have a different genesis.

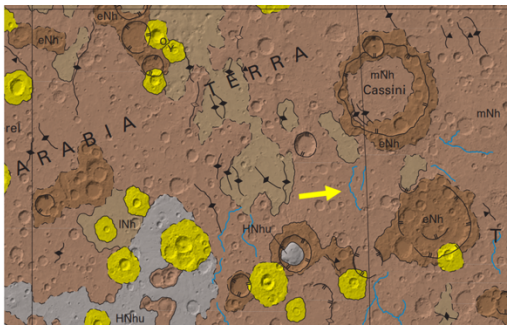

Fig. 1. Geologic map [3] with arrow showing location of Scamander Vallis.

Channel Morphology: Scamander Vallis lies in Arabia Terra, southwest of Cassini Crater (~15ºN, 29ºE) (Fig. 1). The channel lies primarily in middle Noachian terrain, unit mNh [3], and is 260 km long. The channel has several source areas, but the primary is an unnamed Noachian-age crater 40 km in diameter ("A" in Fig. 2). It formerly held a lake that overtopped the northwest crater rim, drained the lake, and eroded the channel. Crater A has a floor at -760 m, but when created would have been much deeper. Correcting for volume effects of craters B and C, the drainable paleolake volume of crater A (above -660 m) was 290 km^3.

The main channel is mildly sinuous and does not branch along its course. It is 260-360 m deep and varies in width from 2.5 to 3.5 km. The channel exhibits a mean slope of 0.003 and additional channel morphology is discussed in Som et al. [4]. The lack of branching along the trunk implies rapid formation of the vallis. At least 100 km^3 of material was eroded to form the vallis. Secondary channels appear along the main channel and, source area excepted, form hanging valleys (Fig. 3, far right).

Channel c1 (Fig. 2) flowed into crater A from a relatively large area south of A. Its floor is deeper than the overtopping level of A, which reveals that the lake extended beyond the crater to lower parts of that area. Prior to breach, the lake volume exceeded that of A.

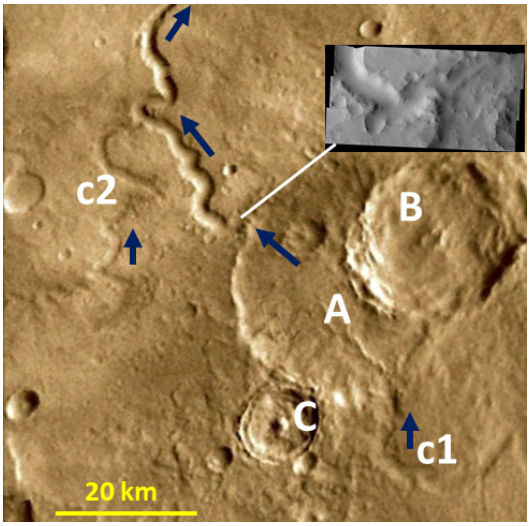

Fig. 2. Source of Scamander Vallis, an unnamed crater (A) with two later, overlapping craters (B & C). Inset at upper right shows where crater lake overtopped rim (Themis V01734006 [5]). Arrows show flow directions in main and secondary channels. Channel c2 likely flowed when c1 flow filled A.

Hydraulic analysis: Using a representative cross-section (MOLA pass 19604) we estimate peak discharge for several scenarios and methods (Table 1).

The crux of discharge estimation is often determining a suitable friction (or roughness) coefficient ('f'). A Darcy-Weisbach formulation is believed to be most reliable [6]. Candidate channel materials in Scamander Vallis include bombardment megaregolith (possibly indurated [7]) and surface dust overlying basalts. Neither depths nor configurations of candidate materials are well-constrained due to aeolian dust cover and low availability of higher resolution DTMs. Here, a range of bed parameters were used to explore outflow.

Bankfull flow scenarios are common in analyses of outburst floods. For unconsolidated gravel beds, discharge varies by a factor of nearly 3. A consolidated bed configuration was also explored. Bed roughness length (k_s) for jointed, columnar basalts was estimated from the Channeled Scablands in Washington [6] and may also reasonably approximate indurated megaregolith (of similar block size). Reynolds number was crudely estimated via Manning equation ('f' is not sensitive to large Re). This scenario yielded similar results as the larger unconsolidated gravel scenarios.

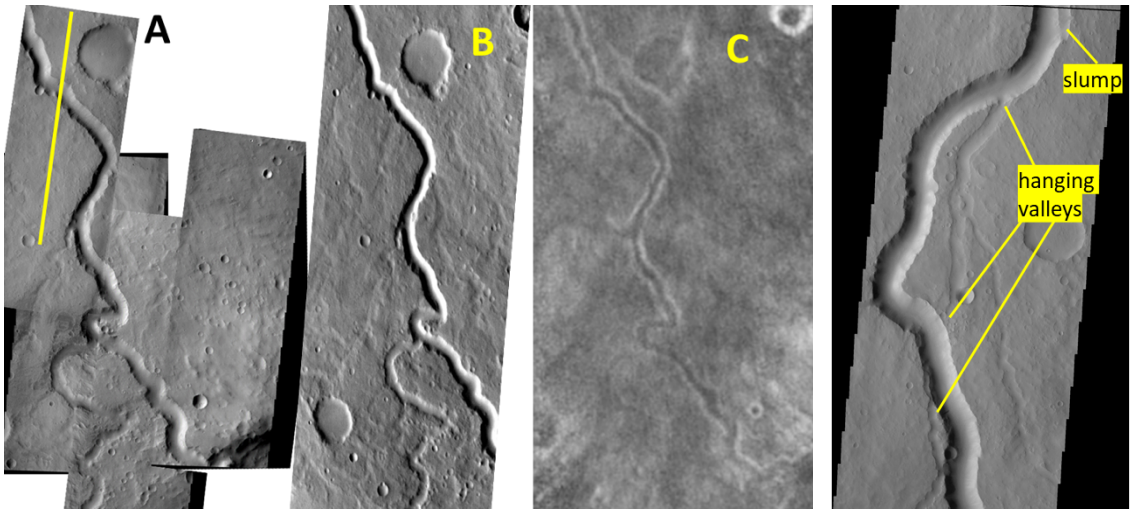

Fig. 3. Comparison of multispectral THEMIS images [5] of southern reaches of Scamander Vallis. Panel A: composite of visible light images that shows crossing (yellow line) of MOLA pass 19064. B: day infrared image I35117006; crater at top is 9 km wide, centered at 15°20'N, 29°2'E. Panel C: night IR composite image. Far right: visible light image (V26845014) of channel showing reaches north of that shown in panels A-C.

Table 1. Peak discharge and velocity estimates in Scamander Vallis.

Scenario	Q_{max} (m^3/s) u_{max} (m/s)	Method & Parameters
Bankfull	6.70E+06 15.6	Modified Manning [8] Assumed n=0.05
Bankfull, gravel bed, D_{90}=0.6 m	4.41E+06 10.2	Darcy-Weisbach via Kleinhans, eq. 13 [9]. f=0.124
Bankfull, gravel bed. D_{84}= 1.0 m	8.87E+06 20.6	Darcy-Weisbach via Wilson et al., eq. 10 [8]. f=0.031
Bankfull, gravel bed. D_{84}=0.1 m	1.19E+07 27.7	Darcy-Weisbach via Wilson et al., eq. 14 [8]. f=0.017
Bankfull, Scabland jointed basalt [6]. D=0.5 m, k_s=20 m	6.77E+06 12.8	Darcy-Weisbach via Colebrook-White [10]. f=0.070
Eroding, Scabland jointed basalt [6]. D=0.5 m, k_s=20 m	1.01E+05 3.6	Darcy-Weisbach via Colebrook-White [10]. f=0.177

Bankfull flows are unlikely (due to extreme bed shear 'τ' and low likelihood of peak discharge after channel completely formed). We adapt a method from Larsen and Lamb [6] for calculating flow in a Scabland-type channel that adjusts as τ exceeds erosion threhold by ~20%. On Mars τ_c is ~40% of that on Earth [11]. From this, active channel geometry and 'f' can be estimated. Peak discharge is more than an order of magnitude less than bankfull scenarios. Bed shear stress from bankfull (1625 Pa) is also significantly greater (288 Pa). The maximum transported fraction was 0.34 (volume of eroded surface materials per volume of drainable water). But this fraction would have been smaller because we find that considerable flow came from the south that drained into crater A.

Conclusions: (1) Scamander Vallis formed primarily via catastrophic flow from a breached crater lake. (2) The unnamed crater filled slowly from the south and overtopped the NW rim. (3) Some secondary channels are hanging valleys at their junction with Scamander. (4) Peak discharge estimates vary by two orders of magnitude, depending on scenario (and, possibly, method of calculating 'f'), with possible overestimation from bankfull scenarios. (5) Improvement in estimates of 'f' and 'Qpeak' requires better understanding of channel/substrate materials. Night THEMIS IR images reveal the Scamander main channel has dust covered slopes. (6) Evidence for a crater lake origin of Scamander Vallis supports the evolving view of a warmer, wetter climate in mid- to late-Noachian time.

References: [1] Carr and Head (2010) *EPSL* ***294***. [2] Davis et al. (2019) *JGR Planets* ***124***. [3] Tanaka, et al. (2014), *USGS Sci. Invest. Map 3292*. [4] Som et al. (2009), *JGR Planets* ***114***. [5] Christensen et al. (2012), THEMIS Data Releases, http://themis-data.asu.edu. [6] Larsen and Lamb (2016), *Nature* ***538***. [7] McEwen et al. (2008), *AGUFM* ***2008***. [8] Wilson et al. (2004), *JGR Planets* ***109***, doi:10.1029/2004JE002281. [9] Kleinhans (2005), *JGR Planets* ***110***. [10] Falvey (1987), *USBR* ***PAP-1156***. [11] Grotzinger et al. (2013), in *Comparative Climatology of Terrestrial Planets* ***Ch. 18***.